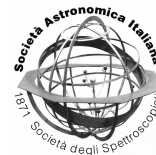




Publication Year	2020
Acceptance in OA @INAF	2022-03-29T10:56:26Z
Title	Modelling anharmonic spectra of Polycyclic Aromatic Hydrocarbons at high temperatures
Authors	MULAS, Giacomo; Chakraborty, S.
Handle	http://hdl.handle.net/20.500.12386/32014
Journal	MEMORIE DELLA SOCIETA ASTRONOMICA ITALIANA



Modelling anharmonic spectra of Polycyclic Aromatic Hydrocarbons at high temperatures

G. Mulas¹ and S. Chakraborty²

¹ Istituto Nazionale di Astrofisica – Osservatorio Astronomico di Cagliari, Via della Scienza 5, 09047 Selargius (CA), Italy, e-mail: giacomo.mulas@inaf.it

² Université de Toulouse – Institut de Recherche en Astrophysique et Planétologie, avenue du Colonel Roche 9, 31028 Toulouse Cedex 4, France

Abstract. Anharmonicity plays a crucial role in determining the band profile and position of the interstellar Polycyclic Aromatic Hydrocarbons. Here we modeled the infrared spectrum of pyrene ($C_{16}H_{10}$) using ab initio simulations. We used our new AnharmoniCaOs code to describe the detailed structures of hot band transitions up to moderately high temperatures (600K), using Monte Carlo sampling of the states but beyond that due to high computational cost it is difficult to extend such fancy calculation up to very high temperature relevant for astrophysics. IR spectra of $C_{16}H_{10}$ beyond 600K was calculated using Density functional based tight binding molecular dynamics simulation. A gradual red shift of the band position and increasing band width is observed with increasing temperatures. The band positions at different temperatures were fitted with a linear regression and the anharmonicity factors were retrieved from the linear fits. Theoretical anharmonicity factors were compared to the recent laboratory results and previous gas phase analyses.

This is an extension of a previous project, aimed at completing the calculations to obtain (relatively) high temperature anharmonic vibrational spectra of the pyrene ($C_{16}H_{10}$) Polycyclic Aromatic Hydrocarbon, using our AnharmoniCaOs code to describe the detailed structures of hot band transitions. We achieved our scientific goal, but the calculation was significantly more demanding than anticipated. The results have been submitted to the Journal of Molecular Spectroscopy by Chakraborty et al., I here describe the technical challenges we faced and the improvements we plan to overcome or mitigate them.

1. Introduction

Polycyclic Aromatic Hydrocarbons (PAHs) are a broad family of molecules composed of fused aromatic rings, whose peripheral bonds are saturated by hydrogen atoms. PAHs (or closely related species) are the most likely carriers of the so-called Aromatic Infrared Bands (AIBs) at $\sim 3.3, 6.7, 7.7, 8.6, 11.3 \mu\text{m}$ (Leger 1984; Allamandola 1985), which are among the strongest emission features observed in

the interstellar medium (Tielens 2008). PAHs in space are excited via electronic transitions in the UV and visible, and re-emit most of this energy in the mid-IR in a vibrational de-excitation cascade. PAHs thus emit most of the flux in the AIBs from highly excited states corresponding to vibrational temperatures of the order of ~ 1000 K (Draine 2011).

Each AIB results from the superposition of the emission of many different molecules at many different temperatures, each of which

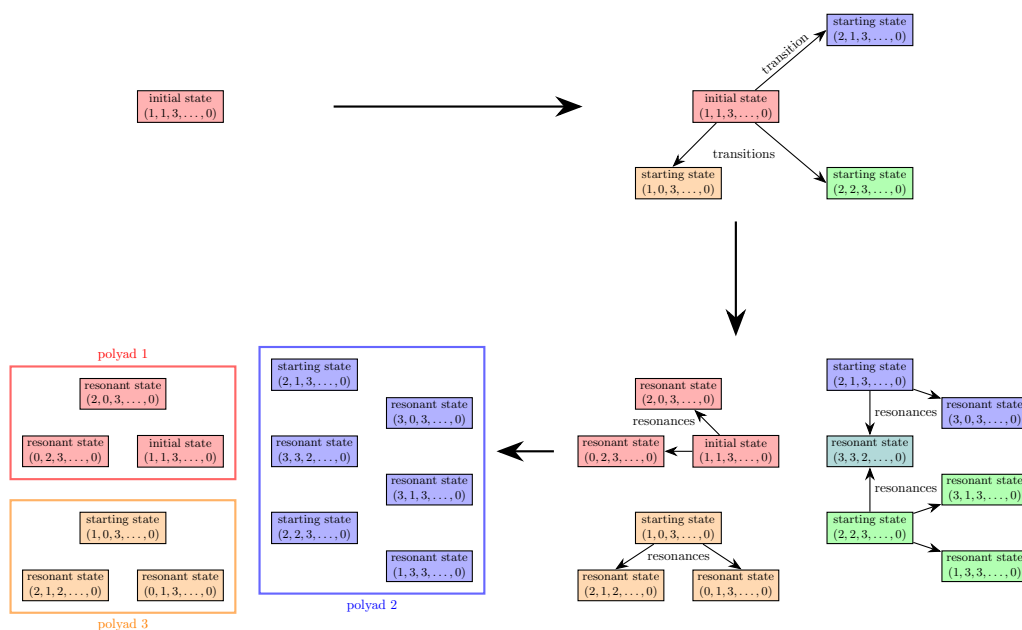


Fig. 1. Schematic algorithm of polyad definition

being the superposition of many vibrational transitions from a statistical distribution of excited states. Each of these individual transitions is slightly shifted by anharmonicity with respect to the corresponding 1-0 fundamental transition, resulting in complex, shifted, and broadened band profiles. Including anharmonicity in AIB models is therefore crucial to link band positions and profiles to the physics of the process of excitation and emission. Our AnharmoniCaOs code¹ implements the generalized second-order vibrational perturbation theory (GVPT2) (Gaw 1991; Martin 1995; Barone 2005; Piccardo 2015) to compute anharmonic vibrational spectra from any arbitrary vibrational state of a given molecule. We exploited this to obtain a Monte Carlo sampling of the vibrational states using the Wang-Landau approach, enabling us to obtain temperature dependent spectra of at finite, non-zero temperatures of Pyrene ($C_{16}H_{10}$) up to ~ 523 K.

This report covers both our previous project CINECA-INAF B18 and the current one, which is its continuation.

2. Computational details

We made use of the Van Vleck approach to perturbation theory applied to molecular vibrations (Sibert 1988a,b; McCoy 1992; Sibert 2013). A simple recap can be found in our paper Mulas (2018). In our previous project we defined the details of the main approximations and truncation strategies employed to make the problem numerically tractable. We also validated method, truncation strategies, and thresholds against high-level calculations on smaller molecules. This has been published in our paper Mulas (2018), as well as calculations for Pyrene ($C_{16}H_{10}$) and Coronene ($C_{24}H_{12}$) at 0K, and comparisons with available experimental data. In this report, we concentrate on the use of our code on Pyrene to derive (relatively) high temperature spectra, more relevant for astronomy.

¹ (<https://sourceforge.net/projects/anharmonica/>)

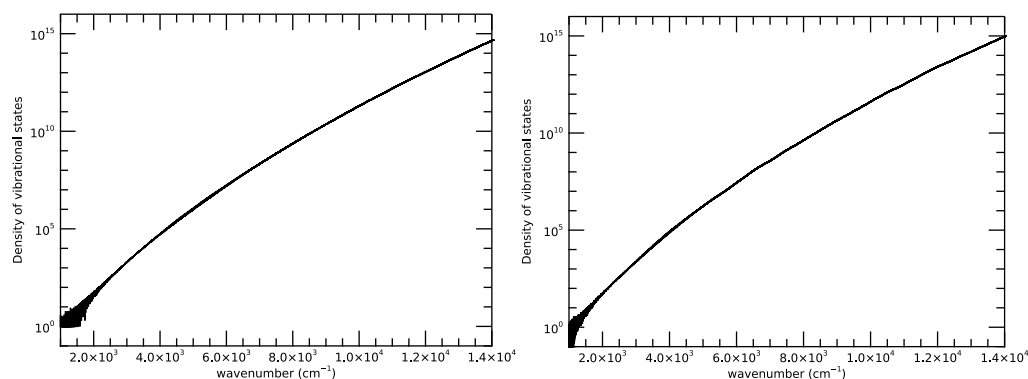


Fig. 2. Left: density of harmonic vibrational states; right: density of anharmonic vibrational states.

The core of the computational burden of this calculation can be divided in four main tasks:

1. initialisation of the code, selection of resonant Hamiltonian terms (to be used to build polyads and effective Hamiltonians in next step) and non-resonant terms, to be included in the perturbative treatment;
2. construction of the polyads and of the corresponding effective Hamiltonians;
3. diagonalisation of the effective Hamiltonians;
4. calculation of the intensities of permitted transitions between diagonalised states.

Step 1 requires a relatively small amount of time, of the order of 1h on a single core. It could conceptually be parallelised in a relatively simple way, but it is not worth the effort, since it needs to be executed only once and for all for a given molecule. It is implemented as a separate code.

Step 2, schematically described in Fig. 1, requires a relatively small amount of time, of the order of 1h on a single core when large polyads are involved. It must be executed for every step of the Wang-Landau random walk or, in general, for each state from which one wants to compute transitions. It is not parallelised, and it would not be trivial to do, since the list of states involved in all polyads would need to be always available to all threads, thus requiring some fairly complex locking and

synchronisations to avoid races. We found it more convenient to also split this to a separate code, which is run as a serial process.

Step 3 is by far the most computationally expensive one. The effective Hamiltonians are sparse matrices, and in principle only a small subset of their eigensolutions are needed, namely the ones which are necessary to cover the vector subspace of the harmonic states we are considering, in each specific iteration of the Wang-Landau random walk to obtain the Monte Carlo sampling of excited states. However, there are no available iterative eigensolvers which are capable to selectively converge on the eigensolutions we want: all known algorithms for the iterative solution of sparse eigenvalue problems select the eigensolutions on the basis of eigenvalues, not of eigenvectors. The implementation of the Jacobi-Davidson method in the SLEPc library (Hernandez 2005, 2003) can be, to some extent, tweaked to favour the eigensolutions we want, but still it turns out to be vastly ineffective compared to standard methods for the complete solution of dense eigenvalue problems. On the other hand, the latter work on dense matrices, hence they require huge amounts of memory to accommodate them: a $100k \times 100k$ matrix in double precision requires of the order of ~ 100 Gbytes just to contain it, the same amount for eigenvectors, and at least as much in working space, possibly quite a bit more depending on the algorithm

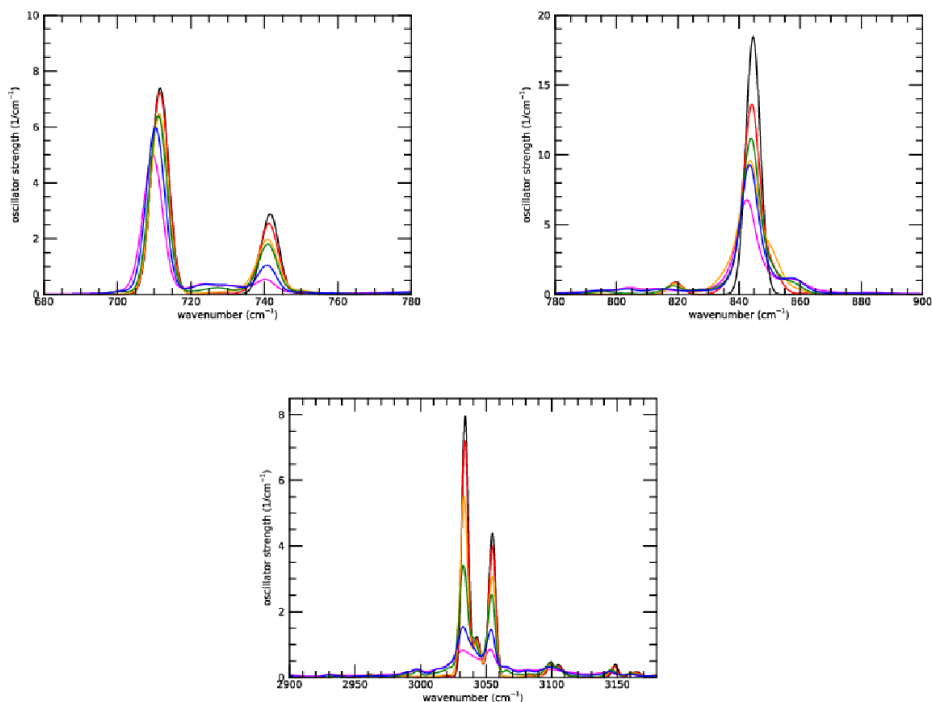


Fig. 3. Some of the strongest fundamental bands of Pyrene, computed for increasing temperatures. Black: 14 K; red: 100 K; orange: 200 K; green: 300 K; blue: 423 K; magenta: 523 K.

used, for a total of >300 Gbytes. This makes it mandatory to use parallel methods working on distributed arrays, e. g. ScaLAPACK (Blackford 1997) or ELPA (Auckenthaler 2011; Marek 2014). Both stock ScaLAPACK and ELPA have problems when dealing with arrays larger than $\sim 32k \times 32k$ elements, and need to be compiled with long integer indices. An implementation of ScaLAPACK using long integer indices is included in the Intel MKL library available on the CINECA machines. We modified ourselves ELPA to include support for long integer indices. The `pdsyevx` ScaLAPACK function turned out to always return complete, correct results. ELPA, while in most cases about twice more efficient than ScaLAPACK, sometimes unpredictably failed to converge gracefully issuing an error

code, while a few times it just hung in endless loops. We submitted error reports to the ELPA developers, together with test code to reproduce them. They acknowledged the problems and replied that they would try to fix them in forthcoming versions of their library. For the present runs, we therefore stuck to ScaLAPACK's `pdsyevx` function, employing up to 32 full nodes of galileo for the largest polyads (mandated by RAM requirements).

Step 4 is not computationally heavy, compared to the previous one. However, since eigenvectors are returned by the previous step in distributed arrays, transition intensities are computed via calls to parallel BLACS functions, also implemented in the Intel MKL libraries available on CINECA machines.

We should mention that, due to symmetry considerations, we partitioned Pyrene transitions in three separate groups that remain completely separated, thereby reducing the size of the polyads and effective Hamiltonians.

Summing up, therefore, the complete project involved the following practical work on CINECA machines:

1. running one serial code once for the initialisation step 1 (repeated for each band type);
2. running a serial code for each step in the Wang-Landau random walk, to build polyads and effective Hamiltonians (step 2 repeated for each band type, hence three times in total);
3. running the parallel code for each step in the Wang-Landau random walk, to diagonalise the effective Hamiltonians and compute transitions among resulting anharmonic states (steps 3 and 4 repeated for each Wang-Landau step and each band type). Each of these parallel processes is run on a number of nodes adequate for RAM requirements.

The preliminary work of defining the steps of the Wang-Landau random walk, as well as post-processing to obtain energy-dependent and temperature-dependent spectra, were performed separately, on local workstations, since they do not require significant computational resources and, conversely, do require significant interactive human intervention.

We remark that determining RAM requirements as a function of polyad size was not trivial: while the standard ScaLAPACK function `pdsyevx` includes the possibility to issue a preliminary call that does no calculations but estimates the size of work space to be allocated, its implementation in the Intel MKL, for efficiency reasons, dynamically allocates additional memory in an undocumented amount, causing the code to just crash during the function call (sometimes a couple of hours into it!) if the allocation fails. We thus had to preliminarily run a small subset of diagonalisations, and derive empirical rules as to the minimum amount of RAM (and hence of full nodes) that is necessary to successfully complete the function call for a given array size.

3. High temperature calculations for Pyrene

Using the Wang-Landau approach in the space of harmonic vibrational states, we obtained a relatively uniform sampling in (harmonic) energy of the vibrational states of Pyrene up to about $11 \times 10^3 \text{ cm}^{-1}$. For each harmonic state, we obtained a distribution of the anharmonic states it contributes to, and their anharmonic energies. Together with the analytic density of harmonic states, this straightforwardly yields the anharmonic density of states. Both harmonic and anharmonic density of states are shown in Figure 2. As already found by previous works (Basire 2009; Parneix 2013), the two densities are very similar, with the anharmonic density curve running more or less parallel to the harmonic one, slightly higher than it. We also obtained uniformly sampled energy-dependent vibrational spectra, from which we can obtain temperature-dependent spectra via a numerical Laplace transform, weighted with the anharmonic density of states. Since we sampled only energies up to a given level, the numerical Laplace transform is accurate only for T low enough to give negligible weight to unsampled energies, which in our case means that we can obtain reliable spectra only up to about $\sim 500 \text{ K}$. Figure 3 shows some of the strongest fundamental bands of Pyrene, computed for a range of temperatures.

The effect of temperature is apparent both in terms of broadening and of position shift. The variation is also clearly stronger for some bands than for others. Some structure which is easily resolved at 14 K is lost at the highest temperatures, and plateaus, composed of very many weak bands getting activated at high temperatures, appear.

Since AnharmoniCaOs also computes overtone, combination, and difference bands, they can also be quantitatively studied. Figure 4 shows two spectral regions in which no fundamental bands are present.

In the region between 2200 and 2400 cm^{-1} no particular bands stand out, but a “carpet” of weak features that, at high temperatures, tend

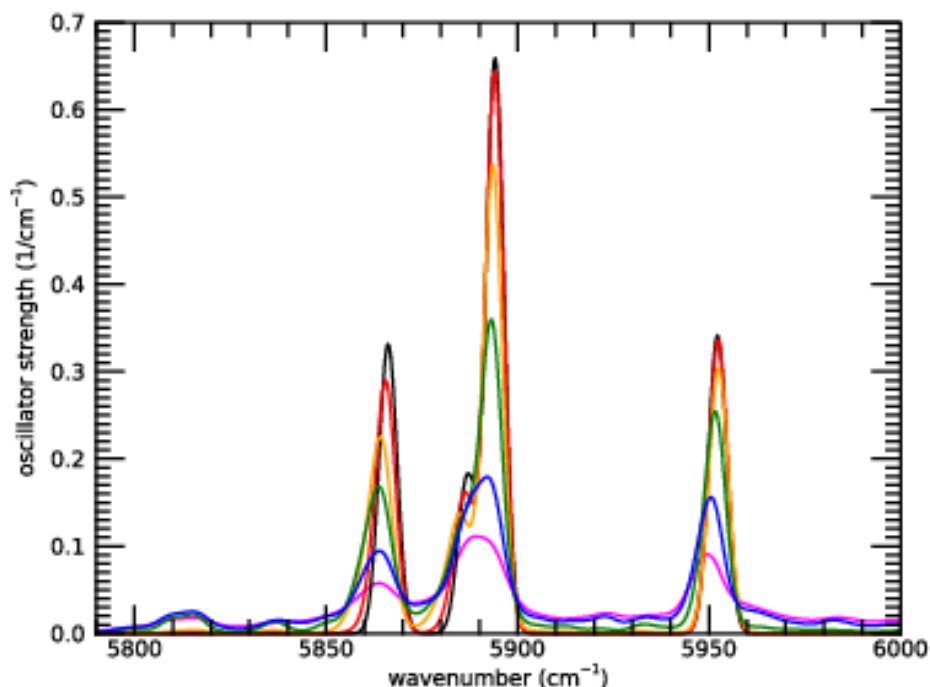


Fig. 4. Combination bands of Pyrene, computed for increasing temperatures. Black: 14 K; red: 100 K; orange: 200 K; green: 300 K; blue: 423 K; magenta: 523 K.

to blend in a pseudo-continuum. Conversely, between 5800 and 6000 cm^{-1} a group of bands clearly stand out, corresponding to the energy of the C-H stretch overtones. Upon closer examination of the calculation, these actually turn out to be dominated not by overtones of the IR-active C-H stretch modes (shown in the lowest panel of Figure 3, but of combination bands of all the C-H stretch modes, including IR-inactive ones. While their integrated total intensity is relatively high, these bands appear to be very strongly broadened with increasing temperatures. Since these bands would require a PAH to be excited to very high vibrational temperatures ($T > 1500$ K) to achieve significant emission, if we extrapolate their behaviour they are likely to be so shallow to be extremely difficult to observe.

4. Discussion and conclusions

We showed that we can indeed quantitatively predict the variation of vibrational band profiles and positions with temperature. We are preparing a publication in which we compare our theoretical calculation with available experimental data, to assess their accuracy (Chakraborty et al. 2021). It is clear from preliminary results that we predict the correct qualitative behaviour, but we still need to check how precisely the calculations match the experiment. As mentioned in the report for the previous project, we are hindered by the lack of eigensolvers tailored to our problem. We are however in the process of rewriting our AnharmoniCaOs code to make it more efficient in two main ways. The first one is to

add a step of sorting, merging, and reordering of the polyads before building the effective Hamiltonians. In this way, if a given polyad appears several times, e. g. once as the lower state of a transition and another as the upper state of another transition, it will be computed only once. The second planned improvement is to try to take advantage of the fact that the states, and the polyads, change gradually along the Wang-Landau random walk among harmonic states. As a consequence, also the corresponding effective Hamiltonians are relatively close between consecutive steps of the random walk. One may therefore use the solutions of the previous step as a “starting point” for the next one, and use an iterative solver instead of the standard Relatively Robust Representations (Dhillon 1997) implemented e. g. in ScaLAPACK. It remains to be seen how effective these changes will prove to be from the computational point of view.

Acknowledgements. We acknowledge the computing centre of Cineca and INAF, under the coordination of the “Accordo Quadro MoU per lo svolgimento di attività congiunta di ricerca Nuove frontiere in Astrofisica: HPC e Data Exploration di nuova generazione”, for the availability of computing resources and support.

References

- Allamandola, L. J., Tielens, A. G. G. M., Barker, J. R. 1985, *ApJ*, 290, L25
- Auckenthaler, T., et al. 2011, *Parallel Comput.*, 37, 783
- Barone, V. 2005, *J. Chem. Phys.*, 122, 014108
- Basire, M., et al. 2009, *J. Phys. Chem. A*, 113, 6947
- Blackford, et al. 1997, *ScaLAPACK Users' Guide* <http://www.netlib.org/scalapack/slug/>
- Chakraborty, S., Mulas, G., Rapacioli, M., et al. 2021, arXiv:2102.06582
- Dhillon, I. 1997, Report n. UCB/CSD-97-971, EECS Department, University of California, Berkeley
- Draine, B.T. 2011, *EAS Publications Series*, 46, 29
- Gaw, F., et al. 1991, in *Advances in Molecular Vibrations and Collision Dynamics: A Research Annual*, ed. J. M. Bowman and M. A. Ratner (JAI Press, Greenwich, Conn.), 1B, 169
- Hernandez, V., Vidal, V. 2003, *Lect. Notes Comput. Sci.*, 2565, 377
- Hernandez, V., Roman, J. E., Vidal, V. 2005, *ACM Trans. Math. Software*, 31, 351
- Léger, A., Puget, J. L. 1984, *A&A*, 137, L5
- Marek, A., et al. 2014, *J. Phys. - Condens. Mat.*, 26, 213201
- Martin, J. M. L., et al. 1995, *J. Chem. Phys.*, 103, 2589
- McCoy, A. B., Sibert, E. L. 1992, *Mol. Phys.*, 77, 697
- Mulas, G., et al. 2018, *J. Chem. Phys.*, 149, 144102
- Parneix, P., Basire, M., Calvo, F. 2013, *J. Phys. Chem. A*, 117, 3954
- Piccardo, M., Bloino, J., Barone, V. 2015, *Int. J. Quantum Chem.*, 115, 948
- Sibert, E. L. 1988a, *J. Chem. Phys.*, 88, 4378
- Sibert, E. L. 1988b, *Comput. Phys. Commun.*, 51, 149
- Sibert, E. L. 2013, *Mol. Phys.*, 111, 2093
- Tielens, A. G. G. M. 2008, *ARA&A*, 46, 289